Neuroscience Letters 757 (2021) 135968

Contents lists available at ScienceDirect

Neuroscience Letters

journal homepage: www.elsevier.com/locate/neulet

Effects of transcranial direct current stimulation on brain network connectivity and complexity in motor imagery

Kangbo Yang [a,b], Xugang Xi [a,b,*], Ting Wang [a,b], Junhong Wang [a,b], Wanzeng Kong [b], Yun-Bo Zhao [c], Qizhong Zhang [a,b]

[a] School of Automation, Hangzhou Dianzi University, Hangzhou 310018, China
[b] Key Laboratory of Brain Machine Collaborative Intelligence of Zhejiang Province, Hangzhou 310018, China
[c] Department of Automation, University of Science and Technology of China, Hefei, 230026, China

ARTICLE INFO

Keywords:
Transcranial direct current stimulation
Electroencephalogram
Primary motor cortex
Supplementary motor area

ABSTRACT

Related experiments have shown that transcranial direct current stimulation (tDCS) anodal stimulation of the brain's primary motor cortex (M1) and supplementary motor area (SMA) can improve the motor control and clinical manifestations of stroke patients with aphasia and dyskinesia. In this study, to explore the different effects of tDCS on the M1 and SMA in motor imagery, 35 healthy volunteers participated in a double-blind randomized controlled experiment. Five subjects underwent sham stimulation (control), 15 subjects underwent tDCS anode stimulation of the M1, and the remaining 15 subjects underwent tDCS anode stimulation of the SMA. The electroencephalogram data of the subjects' left- and right-hand motor imagery under different stimulation paradigms were recorded. We used a functional brain network and sample entropy to examine the different complexities and functional connectivities in subjects undergoing sham-tDCS and the two stimulation paradigms. The results show that tDCS anodal stimulation of the SMA produces less obvious differences in the motor preparation phase, while tDCS anodal stimulation of the M1 produces significant differences during the motor imaging task execution phase. The effect of tDCS on the motor area of the brain is significant, especially in the M1.

1. Introduction

Transcranial direct current stimulation (tDCS) has proven to be an effective tool for regulating cognitive function and brain plasticity [1]. During tDCS, the current is transmitted from the anode to the cathode through the electrode pad placed on the scalp at an intensity of 1–2 mA [1]. As a non-invasive brain stimulation technology, tDCS has attracted much attention because of its potential clinical applications [2]. In recent years, there has been increased research on improving cognition and learning abilities using tDCS [3].

Multiple brain regions, such as the primary motor cortex (M1), premotor cortex, supplementary motor area (SMA), and cerebellum, have been proven to be related to actual motion. The application of tDCS to the M1 has been proven to increase cortical excitability [4] and change plasticity, thereby improving nerve function and motor control [5]. Some brain imaging studies have shown that motor skill learning is also related to brain regions other than the M1, including the SMA [6]. There is effective connectivity between the SMA and M1 [7]. tDCS over the SMA causes excitability changes in the neural structure responsible for pre-motor preparation [8]. This discovery shows that SMA excitability can be modulated externally by tDCS to change motor function in subjects.

However, most research on tDCS of the M1 and SMA focuses on analyzing behavioral data [9] (e.g., improving manual dexterity in sports tasks [10], accuracy of gripping force [11], reaction time [12], and posture control [13]). These studies lack an in-depth analysis of functional connectivity in the brain. Complex brain functions, such as coordinated movement, memory, and language production, rely heavily on dynamic interactions between brain regions [14]. Non-invasive neuromodulators affect the brain network as a whole and do not singularly target the local stimulation site [15]; therefore, we can explore the effect of different electrical stimulation experiments by analyzing the connectivity and complexity of the brain network before and after stimulation. Some experiments have shown that in stroke patients treated with tDCS, the connectivity of the stimulated ipsilateral motor neural network at the alpha frequency of the

* Corresponding author at: School of Automation, Hangzhou Dianzi University, Hangzhou 310018, China.
E-mail address: xixi@hdu.edu.cn (X. Xi).

https://doi.org/10.1016/j.neulet.2021.135968
Received 24 January 2021; Received in revised form 7 May 2021; Accepted 17 May 2021
Available online 21 May 2021

electroencephalogram (EEG) is closely related to changes in corticospinal excitability [16]. This indicates that functional connectivity is a powerful and specific response biomarker [16]. By analyzing the connectivity of the subjects' cerebral cortex in the tDCS experiment, the effect of tDCS can be effectively evaluated.

Motor imagery is an internal representation of a movement that does not involve actual movements in behavior. Because of its beneficial effects in sports rehabilitation training, research on motor imagery has gradually increased. In some experiments of left-right hand motor imagery, applying tDCS to the motor area can lead to changes in the connection between cortical areas [17]. This study explored the different effects of tDCS on brain network connectivity and complexity in the M1 and SMA in motor imagery experiments.

2. Methodology

2.1. Overview

Fig. 1 shows the overview of the methods used in this study. This study mainly used functional brain networks and sample entropy (SampEn) methods to explore the different effects of tDCS on the subjects' M1 and SMA. First, the pre-processed EEG signal was used to calculate the phase synchronization index (PSI) to estimate the correlation between each channel pair to obtain a correlation matrix, as shown in Fig. 1(d). An appropriate threshold (T) was selected to obtain a binary matrix. Further processing of the binary matrix produced a brain network topology map, the average clustering coefficient Fig. 1(c), shortest path length (L), and small-world attributes that characterize brain network features, as shown in Fig. 1(e). In contrast, the pre-processed signal features were extracted using SampEn, which was used for the construction of brain topographic maps, as shown in Fig. 1 (g).

2.2. Experimental procedure

Thirty-five right-handed subjects, including 21 men and 14 women, with an average age of 24 ± 2 years, were included in this experiment. Before the experiment, the subjects were informed in detail about the experimental procedure and possible conditions and provided a signed informed consent form. We conducted a physical examination of the subjects to ensure the safety of the experiment. The survey showed that all the subjects were healthy, had normal vision (with corrective lenses), and had no history of mental illness or other major diseases.

The experimental process was divided into three parts: tDCS, motor imagery task execution, and EEG signal acquisition. A double-blind control experiment was performed for the tDCS. Five subjects underwent sham stimulation (control), 15 subjects underwent tDCS anode stimulation of the M1, and the remaining 15 subjects underwent tDCS anode stimulation of the SMA.

2.2.1. TDCS paradigms

Paradigm 1: The anode was placed over the right M1 (C4), and the cathode was placed on the upper side of the left orbit (FP1).

Paradigm 2: The anode was placed over the right SMA (FC2), and the cathode was placed over the upper side of the FP1.

Electrical stimulation was provided at 1 mA. The duration of the stimulation experiment was 20 min. The electrical stimulation experiments were performed at a fixed time of 9:00 am every day for 3 consecutive days.

2.2.2. Motor imagery task execution

The experimental process is shown in Fig. 2. Before the start of the experiment, the subjects were required to stare at a cross mark displayed on the screen, which was followed by the preparation phase, lasting for a total of 10 s with a corresponding indicator number appearing every 1 s to remind the subjects. The next step was the execution phase of the motor imagery task. This stage lasted for 20 s with upward and

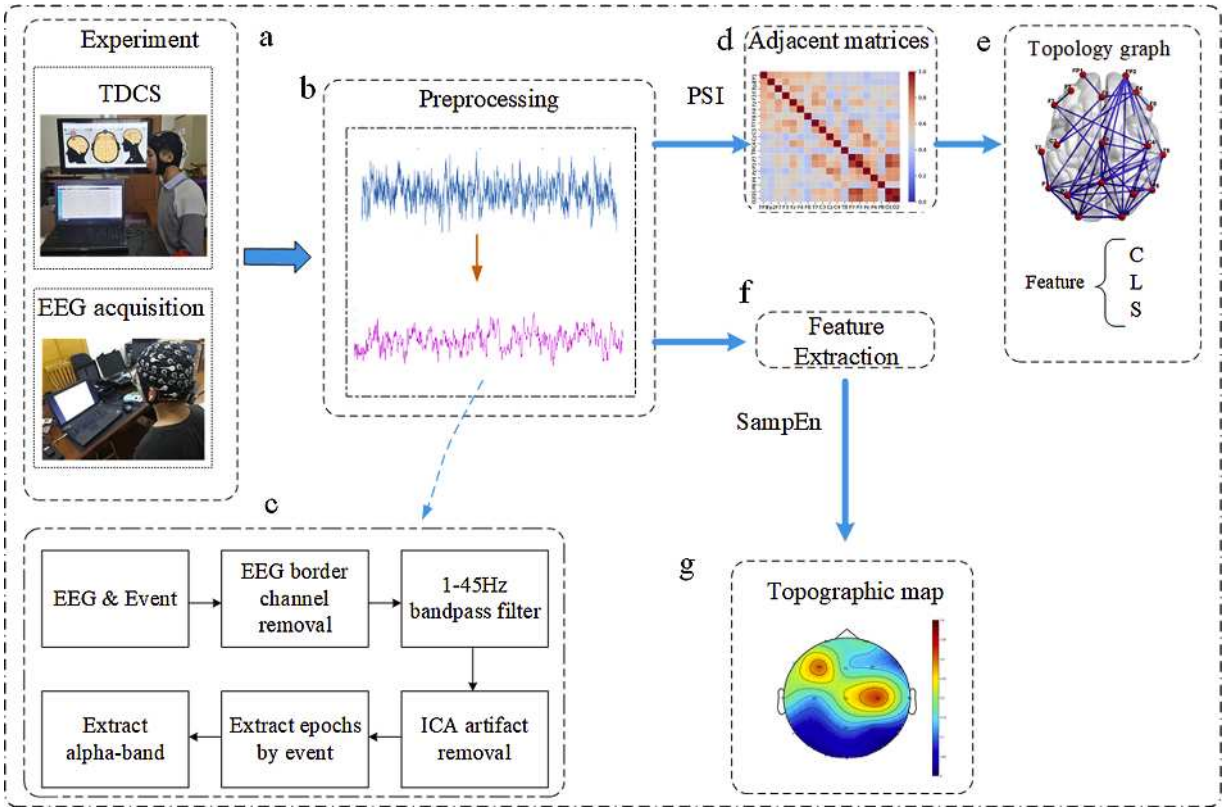

Fig. 1. Schematic diagram of data processing.

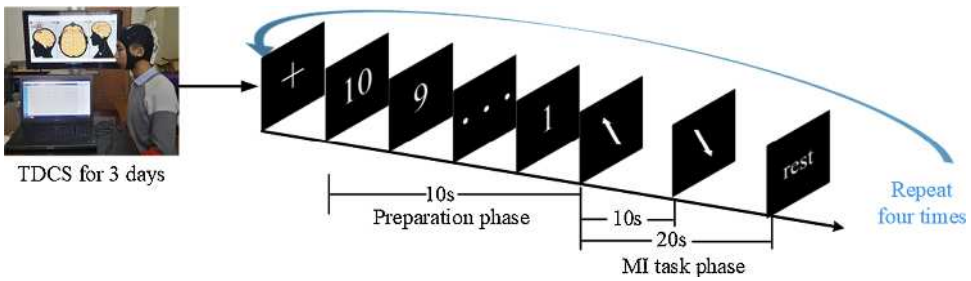

Fig. 2. Experimental process.

downward arrows displayed on the screen, representing imagining making a fist with the left and right hands, respectively. The visualization of each movement lasted 10 s. The subjects repeated the experiment four times, separated by 1-min breaks.

2.2.3. EEG data acquisition and pre-processing

EEG signals were collected in the above preparation and M1 task phases at 9:00 am on the fourth day. The stimulation parameters and sequence of all the subjects during the experiment were the same. All the subjects had no adverse reactions after the completion of the experimental data collection. During data collection, the subjects were required to sit in front of a computer, look at the screen, and perform the corresponding motor imagery task, according to the instructions displayed on the screen.

Data from 35 subjects were recorded. Data from each subject was collected twice in one experiment and 70 pieces of subject data were obtained. A portable wireless EEG amplifier (NeuSen.W64, Neuracle, China) was used for data recording. Electrical stimulation was applied using a StarStim device (Neuroelectrics, Spain). The EEGLAB [18] toolbox in MATLAB (version 2018a; MathWorks) was used to pre-process the EEG signals; the details are shown in Fig. 1(c).

2.3. Data analysis method

2.3.1. Phase synchronization index

The synchronization algorithm based on the Hilbert transform has been widely used in the correlation analysis between multi-channel EEG signals [19]. For a single-channel EEG signal$x(t)$, the analytical signal can be defined as

$$Z(t) = x(t) + j\widetilde{x}(t) = \mathrm{A}_x(t)e^{j\phi_x(t)} \tag{2-1}$$

The PSI of this study was defined as:

$$PSI = \sqrt{< \cos_{\Phi^H_{xy}(t)} >_t^2 + < \sin_{\Phi^H_{xy}(t)} >_t^2} \tag{2-2}$$

where $\Phi_{xy}(t) = \phi_x(t) - \phi_y(t)$ represents the phase difference between the two signals. If$PSI = 0$,$x(t)$ and $y(t)$ are not synchronized, and if$PSI = 1$, then the two signals are completely synchronized.

2.3.2. Sample entropy

An EEG is a nonstationary random signal with typical nonlinear characteristics. Compared with linear models, nonlinear models can better reflect the essence of brain activity; therefore, it is necessary to further explore the effect of tDCS on brain electrical activity from the perspective of the nonlinear dynamics of the EEG. In this study, the SampEn complexity calculation method was used to analyze the effect of tDCS on the nonlinear characteristics of the EEG.

2.3.3. Statistical analysis

In this study, paired *t*-test and double factor analysis of variance were used to test the significance of the difference between sham-tDCS and paradigms 1 and 2. Statistical analyses were performed using SPSS software, version 25 (IBM).

2.4. Network analysis

Fig. 3 shows the correlation matrix constructed using the PSI of the EEG signals for sham-tDCS, paradigm 1, and paradigm 2 in the motor preparation phase and the left- and right-hand motor imagery phases. Blue (PSI = 0) to red (PSI = 1) indicate the lowest and highest correlations, respectively. Sham-tDCS and the two stimulus paradigms showed significant differences in the correlation matrix between the movement preparation and left-right hand motor imagery stages. During the exercise preparation phase, paradigm 2 demonstrated greater synchronization than that observed with sham-tDCS and paradigm 1. The synchronization in paradigm 1 in the execution phase of left-right hand motor imagery tasks, however, was significantly greater than that in sham-tDCS and paradigm 2. In summary, tDCS over the SMA led to greater synchronization than that over the M1 during exercise preparation, while tDCS over the M1 led to greater synchronization than that over the SMA during exercise task execution.

Regarding the selection of the threshold (T), there is currently no unified method [20]. In this study, the multi-threshold method was used to examine changes in network parameters in different experiments. The overall range of T was 0.1–0.75, and the unit step increment was 0.02. A correlation matrix composed of the PSI was converted into an unweighted graph for each subject for each T. The "small-world" (S) characteristics of each unweighted graph were then calculated with the clustering coefficient (C) and feature path length (L).

Some studies have found that complex networks have higher C and shorter L [21], which means that the S attributes are stronger. Fig. 4(a) shows the change in the ratio of C and L with T and that the overall C/L decreases with an increase in the threshold. For smaller thresholds, almost all nodes are connected by edges, and the ratio of clustering coefficient to feature path length changes minimally with an increase in the threshold. As T increases, the connection between the nodes in the network gradually decreases, resulting in a smaller C and increased L. Thus, the C/L value decreases with the increasing threshold.

Fig. 4(a) shows that in the preparation phase, the C/L value of paradigm 2 is the largest when $T > 0.4$, and the difference between paradigms 1 and 2 is small. In the left-right handed execution stage, when the value of C/L changes, the C/L value of paradigm 1 remains the largest. Then, the difference between paradigms 1 and 2 is obvious.

Fig. 4(b) shows that the S attribute change curve leads to a similar conclusion. Since S for the brain network is <1 when the threshold value is >0.5, it does not have the characteristics of a small world and is not shown in the figure.

In addition, we constructed a binary matrix by selecting a fixed threshold (T = 0.55). To visually characterize the connection of brain regions, we drew a network topology diagram corresponding to the binary matrix, as shown in Fig. 5. The brain network topology map was drawn using the MATLAB toolbox BrainNetViewer [22]. The groups of graphs in Fig. 5 show similar organizational structures, but the functional networks after sham-tDCS and the two stimulus paradigms show different regional connectivity.

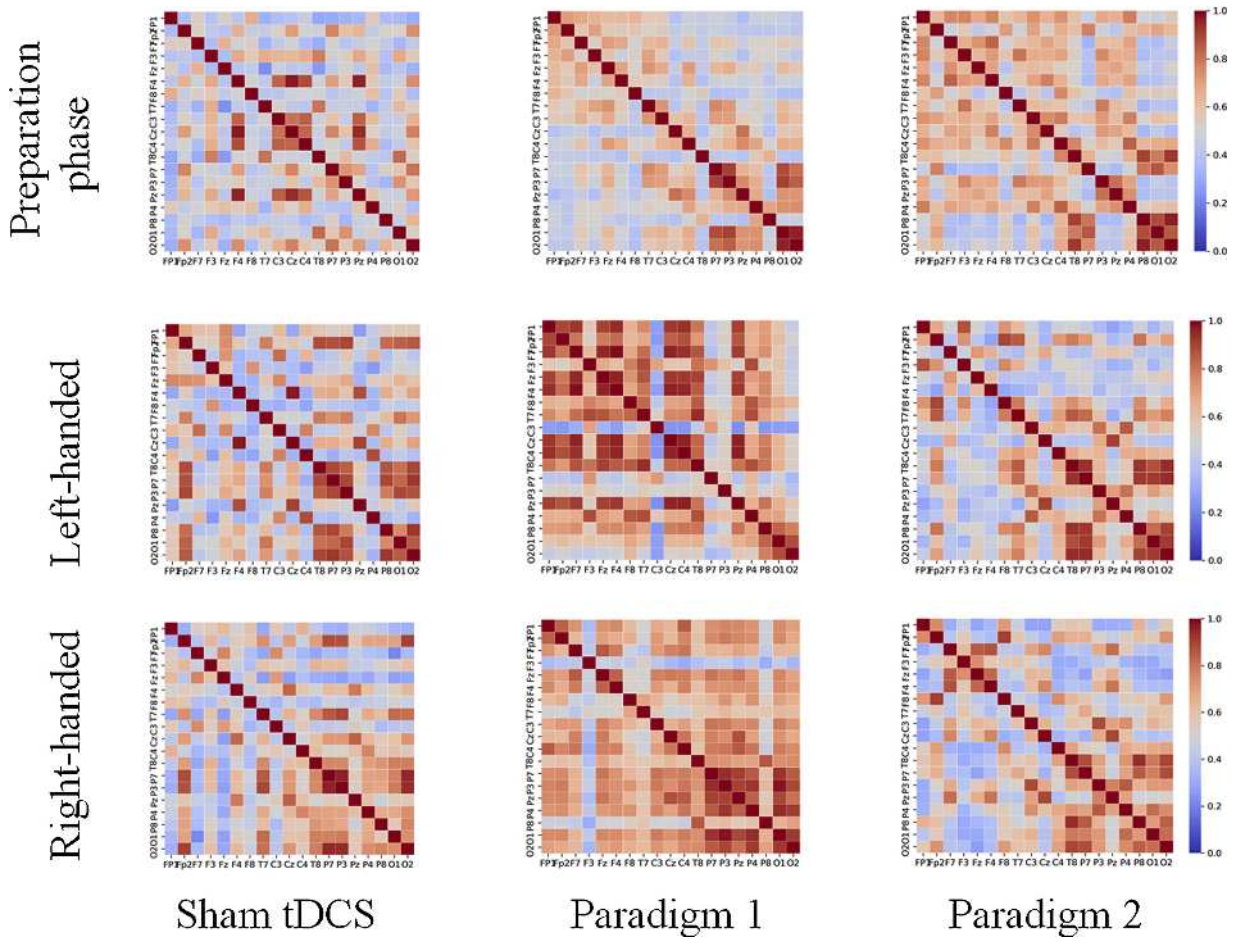

Fig. 3. Correlation matrix constructed using the PSI.

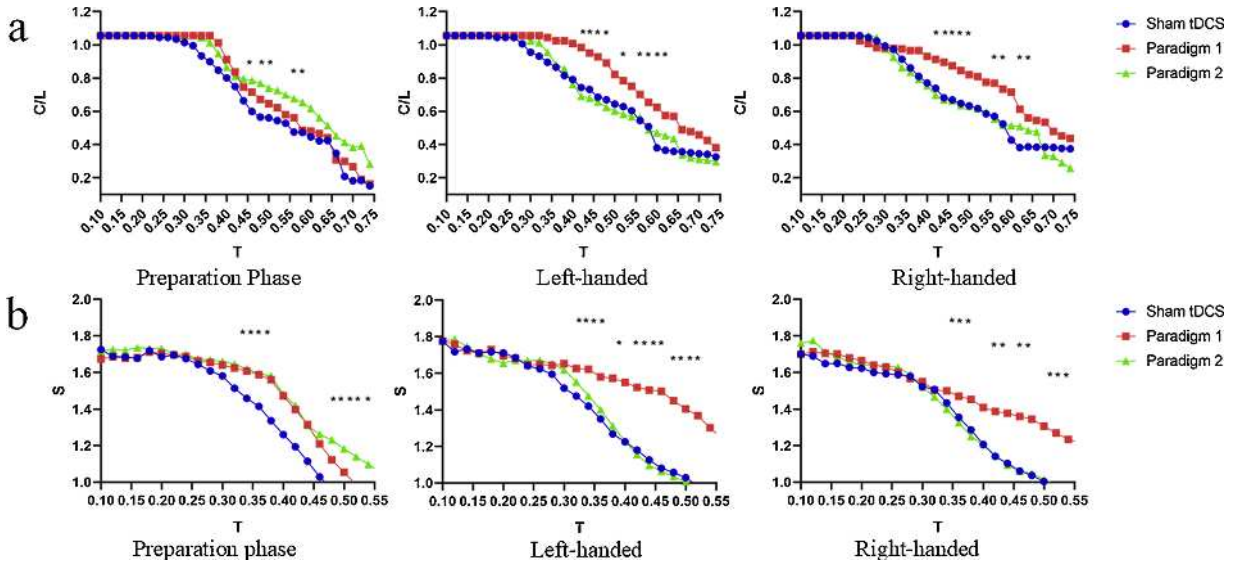

Fig. 4. Brain function network characteristics. * significant difference between the sham stimulus and the two stimulus paradigms (double factor analysis of variance, $p < 0.05$).

2.5. Complexity analysis

In recent years, studies have found that electromagnetic stimulation can cause changes in the nonlinear characteristics of the brain electrical signals of healthy subjects [23], proving that the nonlinear state of the brain may change with external electrical stimulation. This study used SampEn to estimate the regional complexity of EEG signals (Fig. 6). The significance analysis is presented in Table 1.

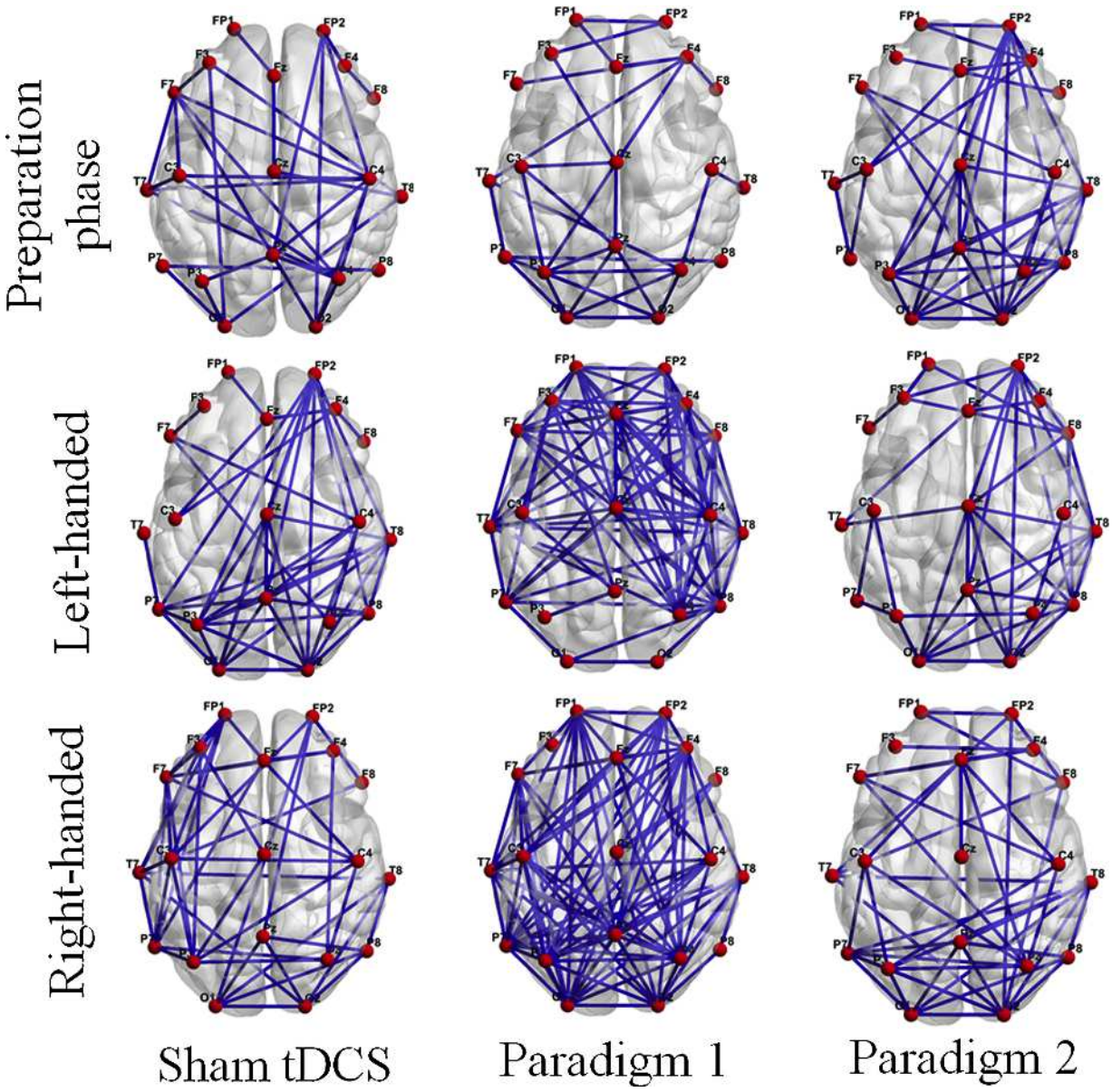

Fig. 5. Topological diagram of the binary matrix.

3. Discussion

In this study, we used functional brain network analysis to study the different effects of tDCS of the M1 and SMA.

The correlation between the EEG signal pathways is shown in Fig. 3. The graph shows that in the exercise preparation phase, the EEG signals in paradigm 2 have a higher correlation. This indicates that in the exercise preparation phase, anodic tDCS over the SMA improves the correlation in subjects' EEG signals better than anodic tDCS over the M1. This supports the conclusions of previous studies [24], showing that the SMA is highly involved in the plan execution phase of autonomous movement [25] and that the application of electric current to the SMA can stimulate the cortical excitability of the corresponding area [26]. Existing evidence shows that complex networks have higher clustering coefficients and shorter feature path lengths [27] or "small world" attributes. This feature makes the network more efficient for the transmission and processing of information. Vecchio et al. [28] found that after being stimulated with bipolar anodal tDCS, the brain network exhibited a "small world" attribute, and the main motor area and related motor areas showed changes in cortical function. We also reached similar conclusions. In Fig. 4, we can see that the brain network after SMA stimulation during the motor preparation phase has a higher "small world" attribute than that after sham-tDCS and M1 stimulation. This shows that the electrical connectivity of the brain can be improved by applying electrical stimulation to the SMA.

In contrast, when performing left-right hand motor imagery tasks, we observed that paradigm 1 exhibited a higher EEG correlation than sham-tDCS and paradigm 2. Stimulation of the M1 with both anodes improved the motor imagery correlation of the EEG channels. Fig. 4 also shows that the "small world" attribute value of the brain after anodal stimulation of the M1 was higher during the execution of the motor imagery task than before anodal stimulation of the SMA. The brain network topology diagram in Fig. 5 shows that the brain regions after anodal stimulation of M1 are relatively tightly connected. However, SMA stimulation did not lead to a significant difference in left- and right-hand motor imagery tasks between subjects. This also shows that the subjects will only show obvious connectivity changes after tDCS of the SMA in the early preparation stage of autonomous movement, while the subjects after tDCS of the M1 will show obvious connectivity throughout the autonomous exercise execution stage.

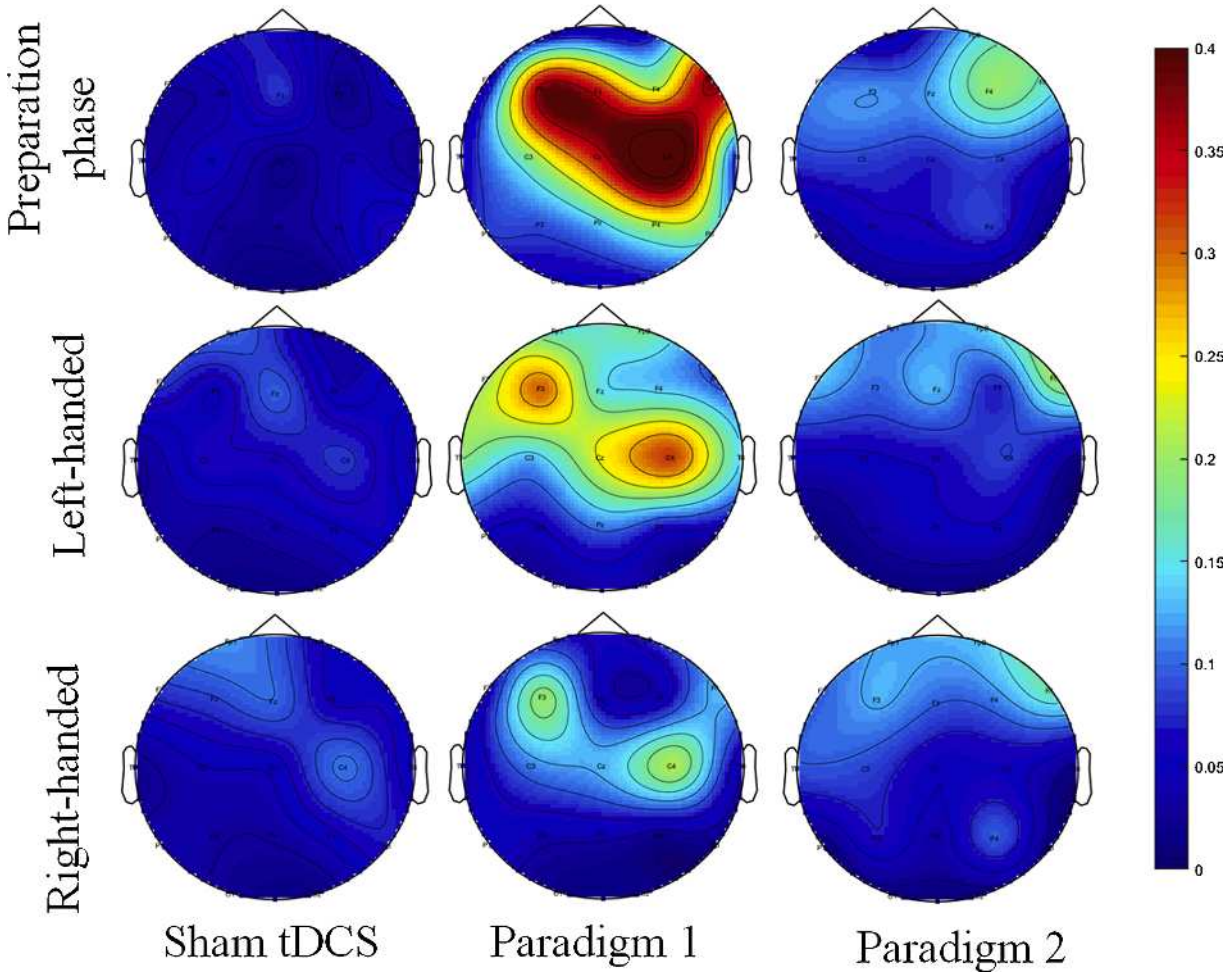

Fig. 6. The SampEn brain topographic map of the EEG signal.

Table 1
Statistical results of SampEn significance test of EEG signals.

	Preparation phase	Left-handed	Right-handed
Sham-tDCS & Paradigm 1	<0.001**	0.001*	0.285
Sham-tDCS & Paradigm 2	0.018*	0.48	0.060

Paired *t*-test.
* $p < 0.05$.
** $p < 0.001$.

We found different phenomena when we further calculated the complexity of the EEG signals using SampEn. Overall, the two stimulus paradigms can increase the complexity of the subjects' EEG signals, especially during the exercise preparation stage. However, in the execution stage of the motor imagery task, the increase in complexity was not obvious, and there was no significant difference in the increase in complexity during the right-hand motor imagery task (paradigm 1 = 0.060; paradigm 2 = 0.385). This is slightly different from the conclusions we obtained from the brain network analysis. Studies have shown that complexity increases when the subject is in a state of tension or alertness [29]. Since the screen continuously reminds the subject to prepare based on the countdown number displayed during the exercise preparation stage, we suggest that the subject has entered a state of alertness at this stage, resulting in higher complexity. The complexity did not change significantly in the control group.

The number of subjects who underwent sham stimulation was relatively smaller than that of subjects who underwent tDCS of the M1 and SMA. To eliminate bias, the number of subjects must be increased. In addition, the subjects recruited in this study were all young people, and their age distribution was not representative.

4. Conclusion

In this study, the graph theory was used to construct a functional brain network to obtain the network features. Through analysis of the network features, we found that the effect of tDCS on the SMA was more obvious in the motor preparation stage, but not throughout the entire motor imagery task execution stage. The effect of tDCS on the M1 is opposite. The effect of tDCS is more obvious in the execution of the entire motor imagery task, but not in the motor preparation stage.

CRediT authorship contribution statement

Kangbo Yang: Methodology, Software, Data curation. **Xugang Xi:** Conceptualization, Project administration. **Ting Wang:** Writing - original draft. **Junhong Wang:** Software, Visualization. **Wanzeng Kong:** Software, Validation. **Yun-Bo Zhao:** Supervision, Formal analysis. **Qizhong Zhang:** Resources.

Acknowledgements

This work was supported by the National Natural Science Foundation of China (Nos. 61971169, 62061044 and 60903084), and Zhejiang Provincial Key Research and Development Program of China (No. 2021C03031), Zhejiang Provincial Natural Science Foundation of China (NO. LQ21H180005), and Fundamental Research Funds for the

Provincial Universities of Zhejiang (NO. GK199900299012-016).

References

[1] D. Cappon, M. Jahanshahi, P. Bisiacchi, Value and efficacy of transcranial direct current stimulation in the cognitive rehabilitation: a critical review since 2000, Front. Neurosci. 10 (2016), https://doi.org/10.3389/fnins.2016.00157.

[2] N.S. Philip, B.G. Nelson, F. Frohlich, K.O. Lim, A.S. Widge, L.L. Carpenter, Low-intensity transcranial current stimulation in psychiatry, Am. J. Psychiatry 174 (2017) 628–639, https://doi.org/10.1176/appi.ajp.2017.16090996.

[3] B. Hordacre, B. Moezzi, M.C. Ridding, Neuroplasticity and network connectivity of the motor cortex following stroke: a transcranial direct current stimulation study, Hum. Brain Mapp. 39 (2018) 3326–3339, https://doi.org/10.1002/hbm.24079.

[4] M.A. Nitsche, W. Paulus, Sustained excitability elevations induced by transcranial DC motor cortex stimulation in humans, Neurology 57 (2001) 1899–1901, https://doi.org/10.1212/WNL.57.10.1899.

[5] A.M. Goodwill, J. Reynolds, R.M. Daly, D.J. Kidgell, Formation of cortical plasticity in older adults following tDCS and motor training, Front. Aging Neurosci. 5 (2013) 1–9, https://doi.org/10.3389/fnagi.2013.00087.

[6] E. Dayan, L.G. Cohen, Neuroplasticity subserving motor skill learning, Neuron 72 (2011) 443–454, https://doi.org/10.1016/j.neuron.2011.10.008.

[7] M. Vassal, C. Charroud, J. Deverdun, E. Le Bars, F. Molino, F. Bonnetblanc, A. Boyer, A. Dutta, G. Herbet, S. Moritz-Gasser, A. Bonafé, H. Duffau, N.M. De Champfleur, Recovery of Functional Connectivity of the Sensorimotor Network After Surgery for Diffuse Low-Grade Gliomas Involving the Supplementary Motor Area, 2017, https://doi.org/10.3171/2016.4.JNS152484.

[8] A.N. Carlsen, J.S. Eagles, C.D. MacKinnon, Transcranial direct current stimulation over the supplementary motor area modulates the preparatory activation level in the human motor system, Behav. Brain Res. 279 (2015) 68–75, https://doi.org/10.1016/j.bbr.2014.11.009.

[9] R. Hannah, A. Iacovou, J.C. Rothwell, Direction of TDCS current flow in human sensorimotor cortex influences behavioural learning, Brain Stimul. 12 (2019) 684–692, https://doi.org/10.1016/j.brs.2019.01.016.

[10] B.W. Vines, C. Cerruti, G. Schlaug, Dual-hemisphere tDCS facilitates greater improvements for healthy subjects' non-dominant hand compared to uni-hemisphere stimulation, BMC Neurosci. 9 (2008) 1–7, https://doi.org/10.1186/1471-2202-9-103.

[11] S. Miyaguchi, N. Otsuru, S. Kojima, H. Yokota, K. Saito, Y. Inukai, H. Onishi, Gamma tACS over M1 and cerebellar hemisphere improves motor performance in a phase-specific manner, Neurosci. Lett. 694 (2019) 64–68, https://doi.org/10.1016/j.neulet.2018.11.015.

[12] H. Sugata, K. Yagi, S. Yazawa, Y. Nagase, K. Tsuruta, T. Ikeda, K. Matsushita, M. Hara, K. Kawakami, K. Kawakami, Modulation of motor learning capacity by transcranial alternating current stimulation, Neuroscience 391 (2018) 131–139, https://doi.org/10.1016/j.neuroscience.2018.09.013.

[13] E. Saruco, F. DI Rienzo, S. Nunez-Nagy, M.A. Rubio-Gonzalez, P.L. Jackson, C. Collet, A. Saimpont, A. Guillot, Anodal tDCS over the primary motor cortex improves motor imagery benefits on postural control: a pilot study, Sci. Rep. 7 (2017) 1–9, https://doi.org/10.1038/s41598-017-00509-w.

[14] C. Peña-Gómez, R. Sala-Lonch, C. Junqué, I.C. Clemente, D. Vidal, N. Bargalló, C. Falcón, J. Valls-Solé, Á. Pascual-Leone, D. Bartrés-Faz, Modulation of large-scale brain networks by transcranial direct current stimulation evidenced by resting-state functional MRI, Brain Stimul. 5 (2012) 252–263, https://doi.org/10.1016/j.brs.2011.08.006.

[15] W.T. To, D. De Ridder, J. Hart, S. Vanneste, Changing brain networks through non-invasive neuromodulation, Front. Hum. Neurosci. 12 (2018) 1–17, https://doi.org/10.3389/fnhum.2018.00128.

[16] E. Welsby, M. Ridding, S. Hillier, B. Hordacre, Connectivity as a predictor of responsiveness to transcranial direct current stimulation in people with stroke: protocol for a double-blind randomized controlled trial, JMIR Res. Protoc. 7 (2018) e10848, https://doi.org/10.2196/10848.

[17] B.S. Baxter, B.J. Edelman, A. Sohrabpour, B. He, Anodal transcranial direct current stimulation increases bilateral directed brain connectivity during motor-imagery based brain-computer interface control, Front. Neurosci. 11 (2017) 1–17, https://doi.org/10.3389/fnins.2017.00691.

[18] A. Delorme, T. Mullen, C. Kothe, Z. Akalin Acar, N. Bigdely-Shamlo, A. Vankov, S. Makeig, EEGLAB, SIFT, NFT, BCILAB, and ERICA: new tools for advanced EEG processing, Comput. Intell. Neurosci. 2011 (2011), https://doi.org/10.1155/2011/130714.

[19] C.J. Stam, G. Nolte, A. Daffertshofer, Phase lag index: assessment of functional connectivity from multi channel EEG and MEG with diminished bias from common sources, Hum. Brain Mapp. 28 (2007) 1178–1193, https://doi.org/10.1002/hbm.20346.

[20] C.J. Stam, W. De Haan, A. Daffertshofer, B.F. Jones, I. Manshanden, A.M. Van Cappellen Van Walsum, T. Montez, J.P.A. Verbunt, J.C. De Munck, B.W. Van Dijk, H.W. Berendse, P. Scheltens, Graph theoretical analysis of magnetoencephalographic functional connectivity in Alzheimer's disease, Brain 132 (2009) 213–224, https://doi.org/10.1093/brain/awn262.

[21] H. Wang, W. Chang, C. Zhang, Functional brain network and multichannel analysis for the P300-based brain computer interface system of lying detection, Expert Syst. Appl. 53 (2016) 117–128, https://doi.org/10.1016/j.eswa.2016.01.024.

[22] M. Xia, J. Wang, Y. He, BrainNet viewer: a network visualization tool for human brain connectomics, PLoS One 8 (2013), https://doi.org/10.1371/journal.pone.0068910.

[23] D. Zhou, J. Zhou, H. Chen, B. Manor, J. Lin, J. Zhang, Effects of transcranial direct current stimulation (tDCS) on multiscale complexity of dual-task postural control in older adults, Exp. Brain Res. 233 (2015) 2401–2409, https://doi.org/10.1007/s00221-015-4310-0.

[24] R. Romo, W. Schultz, Neuronal activity preceding self-initiated or externally timed arm movements in area 6 of monkey cortex, Exp. Brain Res. 67 (1987) 656–662, https://doi.org/10.1007/BF00247297.

[25] P.E. Roland, B. Larsen, N.A. Lassen, E. Skinhoj, Supplementary motor area and other cortical areas in organization of voluntary movements in man, J. Neurophysiol. 43 (1980) 118–136, https://doi.org/10.1152/jn.1980.43.1.118.

[26] T. Furubayashi, Y. Terao, N. Arai, S. Okabe, H. Mochizuki, R. Hanajima, M. Hamada, A. Yugeta, S. Inomata-Terada, Y. Ugawa, Short and long duration transcranial direct current stimulation (tDCS) over the human hand motor area, Exp. Brain Res. 185 (2008) 279–286, https://doi.org/10.1007/s00221-007-1149-z.

[27] B.S. Baxter, B. Edelman, X. Zhang, A. Roy, B. He, Simultaneous high-definition transcranial direct current stimulation of the motor cortex and motor imagery, 2014 36th Annu. Int. Conf. IEEE Eng. Med. Biol. Soc. EMBC 2014 (2014) 454–456, https://doi.org/10.1109/EMBC.2014.6943626.

[28] F. Vecchio, R. Di Iorio, F. Miraglia, G. Granata, R. Romanello, P. Bramanti, P. M. Rossini, Transcranial direct current stimulation generates a transient increase of small-world in brain connectivity: an EEG graph theoretical analysis, Exp. Brain Res. 236 (2018) 1117–1127, https://doi.org/10.1007/s00221-018-5200-z.

[29] X.S. Zhang, R.J. Roy, E.W. Jensen, EEG complexity as a measure of depth of anesthesia for patients, IEEE Trans, Biomed. Eng. 48 (2001) 1424–1433, https://doi.org/10.1109/10.966601.